ASIAN JOURNAL OF PHARMACEUTICAL AND CLINICAL RESEARCH

INNOVARE ACADEMIC SCIENCES
Knowledge to Innovation

Vol 8, Issue 1, 2015

ISSN - 0974-2441

Research Article

PREPARATION AND INITIAL BIOCOMPATABILITY EVALUATION OF BIOGENIC HYDROXYAPATITE/CHITOSAN/POLYVINYL ALCOHOL BIOCOMPOSITE AS A DRUG DELIVERY CARRIER OF PRONEUROGENIC FACTOR

JAYSHREE NELLORE*, VIJAYALAKSHMI S, PENUBOLO PRIYANKA, STUTI PRIYADARSHINI

Department of Biotechnology, Sathyabama University, Chennai - 600 119, Tamil Nadu, India. Email: sree_nellore@yahoo.com

Received: 23 October 2014, Revised and Accepted: 21 November 2014

ABSTRACT

Objective: This study explores the synthesis of biogenic hydroxyapatite (HAp)/chitosan (CS)/polyvinyl alcohol (PVA) bio-composites for delivery of proneurogenic factor, retinoic acid for reconstruction of craniofacial deformities.

Methods: In order to accomplish this aim, we started with the synthesis of HAp using the biomolecules occluded in the cucumber peel (CPHAp). Scanning electron microscopy (SEM), Fourier transform infrared spectroscopy (FTIR) and X-ray diffraction studies (XRD) studies confirmed the purity and morphology of CPHAp. Further, a microenvironment for nerve cell growth was designed by synthesis of biogenic HAp/CS/PVA blends loaded with retinoic acid (CS-PVA-CPHAp-all-trans-retinoic acid [ATRA]). The prepared biocomposites were characterized under advanced analytical instruments such as SEM, FTIR, and XRD.

Results: The SEM analysis for the prepared biocomposites confirmed the formation of interconnected porous matrix. The results of FTIR confirm the biocomposite formation without chemical modification of ATRA. From XRD the amorphous nature was confirmed, inducing suitability of the material for delivery process. Release of ATRA from CS-PVA-CPHAp-ATRA was sustained, with a cumulative release of 55% at the end of 10th day. Furthermore, 3-(4, 5-dimethylthiazol-2-yl)-2, 5-diphenyltetrazolium bromide assay indicated that, the biocomposites are better in scaffold properties, and it provides a healthier environment for cell attachment and spreading.

Conclusion: The porous CS-PVA CPHAp-ATRA composites may be applied to craniofacial tissue engineering as a long-term or permanent scaffold due to their good biocompatibility and sustained release of proneurogenic factor.

Keywords: Hydroxyapatite/chitosan/polyvinyl alcohol bio-composites, Biocompatibility, Cell compatibility, Scaffold, Craniofacial deformities.

INTRODUCTION

Injuries caused by trauma, tumor or cyst resection, infectious diseases, and also congenital and developmental conditions results in craniofacial deformities [1]. Novel tissue engineering therapies aimed at enabling clinicians to achieve predictable regeneration through the use of biomaterial scaffolds that can mimic the microenvironment present in healthy tissue [2].

Since the craniofacial regions are innervated by the body's most sophisticated nerve fibers the main role of the scaffold is to provide a structure that is permissive for axon growth and maintain their proliferation [3]. Recent works suggest that the retinoic acid provides correct guidance to the peripheral nerve innervations and regeneration of lost structures [4].

Now-a-days, great attention is focused on polymer/ceramic three-dimensional scaffolds favoring craniofacial bone regeneration. Several studies have focused on the composite scaffold for craniofacial bone tissue engineering [5], such as chitosan (CS)/calcium phosphate [6], CS/hydroxyapatite (HAp) bilayer scaffold [7]. It was also found that when they are joined to synthetic polymers such as polyvinyl alcohol (PVA) they increase the mechanical properties of the resulting materials [8]. These biopolymers have received various advantages in the recent years as researchers continue to investigate and modify these biomaterials for demanding needs of biomedical applications in the drug delivery.

Tan *et al*., 2009 prepared thermo-sensitive CS/PVA hydrogels containing HAp for protein delivery [9]. Celebi *et al*., 2013 developed electrospun CS/PVA nanofibers containing silver incorporated HAp nanoparticles, which exhibited antibacterial efficiency against *Escherichia coli* [10]. Despite the widespread use of materials in tissue engineering, many biomaterials lack the desired functional properties to provide correct guidance to the peripheral nerve innervations and regeneration of lost structures.

With the ever-increasing requirement of artificial replacements, there is a need for constant innovation in the biomaterials field. In addition, there is an ever-growing need to develop clean, non-toxic and environmentally friendly (green nanotechnology) procedure for nanoparticle synthesis [11]. The biomimetic synthesis of inorganic particles using known matrices is already well established, however, there are only a few reports using compound extracts. Nayar and Guha, 2009, have used several biomolecules (from waste materials like orange and potato peel, eggshell and also medicinally important substances like papaya leaf and calendula flower extract) for the *in situ* synthesis of HAp [12].

Keeping the above facts in view, we started with the synthesis of HAp using the biomolecules occluded in the cucumber peel. Further, a microenvironment permissive for peripheral nerve innervations and regeneration of lost structures nerve cell growth was designed by synthesis of biogenic HAp/CS/PVA blends loaded with retinoic acid.

METHODS

Materials

For *in situ* synthesis of HAp nanocomposites cucumber peel was collected from kitchen waste.

Other chemicals required for various experimental procedures *viz*., hydrochloric acid, 0.156M alkaline diammonium hydrogen phosphate,

25% liquor ammonia, alkaline calcium nitrite tetrahydrate, 1% acetic acid, 1% tripolyphosphate, retinoic acid, ethanol, PVA, ethylene diamine tetra acetic acid etc., were procured from sigma.

Methods

In situ synthesis of HAp from cucumber peels (CPHAp)

In situ synthesis of HAp was carried out according to the methods described by Nayar and Guha, 2009 [12]. 4 g of cucumber peel was boiled in water for 10 minutes and then filtered. To 60 ml of this filtrate, 700 ml of 0.4 M alkaline calcium nitrite tetrahydrate solution and 100 ml of (1:2) liquor ammonia (25%): H_2O was added, mixed thoroughly and incubated for 24 hrs at 30°C. The resulting solution was added to 800 ml 0.156 M alkaline diammonium hydrogen phosphate salt solution, stirred and aged for 1 week at an ambient temperature of 30°C. After this, the precipitate was washed several times with de-ionized water and oven dried at 80°C.

Characterization of CPHAp

X-ray diffraction (XRD) was done using (Siemens, D500) with Cu Kα radiation at 30 kV and 25 mA scanned for diffraction angles: 2θ - 20-80°, at room temperature. Scanning electron microscopy (SEM) studies were done using (JEOL 840). The synthesized powders were mounted on a brass staff, and gold coated and images recorded at 20 KV. Fourier transforms infrared (FTIR) spectra were obtained in the region 400-4000/cm from the powdered samples mixed with KBr.

Fabrication of blank and encapsulated biocomposite

The biocomposite was prepared using a modified protocol as explained previously [9]. A 3% CS was prepared by dissolving CS in 1N acetic acid. The solution was homogenized stirring overnight at room temperature, and the undissolved polymers were removed by filtration. Then, it was poured into a regulator container having PVA solution, which was previously dissolved in the same solvent at 95°C and under magnetic stirring for 3 hrs. The concentration of PVA and CS were 7% and 3%, respectively before mixing process. All-trans-retinoic acid (ATRA) was firstly dissolved in methanol (0:1 mg/ml) and then thoroughly mixed with cooled CS-PVA slurry for 10 minutes. CP-HAp form cucumber peel was suspended in the above solvent system and exposed to ultrasound for 30 minutes to finalize the CS-PVA-CP-HAp-ATRA blend. The concentration of HA in the mixture was 2 w/v% of total solvent system. The thus obtained slurry was loaded into a cylindrical mold and allowed to freeze dry to obtain CS-PVA-HAp composite matrices encapsulated with ATRA (CS-PVA-CPHAp-ATRA). Blank composite matrices (CS-PVA-CPHAp) were fabricated without the addition of ATRA.

Characterization of blank and encapsulated biocomposites

XRD was done using (Siemens, D500) with Cu Kα radiation at 30 kV and 25 mA scanned for diffraction angles: 2θ −20-80°, at room temperature. SEM studies were done using (JEOL 840). The synthesized powders were mounted on a brass staff, and gold coated and images recorded at 20 KV. FTIR spectra were obtained in the region 400-4000/cm from the powdered samples mixed with KBr.

Encapsulation efficiency studies

A total of 0.3 g of accurately weighed CS-PVA-CPHAp-ATRA biocomposite was transferred with precaution to a volumetric flask containing 100 ml of artificial cerebrospinal fluid (pH=7.4, ionic strength 0.01 at 30°C) and kept overnight with continuous stirring to dissolve the ATRA in the matrices. The solution was allowed to settle down, filtered, and collected. The ATRA inside the biocomposite matrices was determined, employing ultraviolet (UV) spectrophotometer. The loading efficiency (%) was calculated by using a calibration curve and the following formula. Loading efficiency (%) = $W_1/W_2 \times 100$

Where

Nomenclature

W_1 amount of ATRA encapsulated in a known amount of matrices,

W_2 weight of matrices.

***In vitro* release studies**

ATRA release studies from the CS-PVA-CPHAp-ATRA biocomposite was carried out with the help of absorbance readings by using UV-visible (UV-Vis) spectrophotometer (UV-2001 Hitachi); 0.3 g of the biocomposite was taken into a known volume (100 ml) of dissolution media (pH=1.2 and 7.4). The pH of the medium was maintained by using hydrochloric acid and phosphate buffer solution. The content was shaken from time to time, and the temperature maintained throughout was 30°C (room temperature). An aliquot sample of known volume (5 ml) was removed at appropriate time intervals, filtered, and assayed spectrophotometrically at 261 nm for the determination of the cumulative amount of drug release up to a time-t. Each determination was carried out in triplicate. To maintain a constant volume, 5 ml of the dissolution medium was returned to the container.

3-(4, 5-dimethylthiazol-2-yl)-2, 5-diphenyltetrazolium bromide (MTT) assay for cell activity studies

Cell activity studies were conducted using vero cell lines as described by Song *et al*., 2012 with slight modifications [8]. The viability of the cells grown on the biocomposites was determined using the colorimetric MTT assay. For the assay, cells were then seeded onto 96 well plates at a density of 10^4 cells/well and were incubated under standard culturing conditions. Extract from the biocomposites was prepared by incubating the pre-sterilized biocomposites incubated in culture medium and the medium with leachable was collected in a falcon tube. Culture media of the seeded cells were replaced after 24 hrs by the extract (media with the leachable). Cells were incubated on the extract for 24 and 48 hrs. After an incubation period, the extract was replaced by fresh media containing 10% of MTT solution. Then the plates were incubated at 37°C in humidified atmosphere for 4 hrs. The formazan crystals formed were solubilized in dimethyl sulfoxide and read at 590 nm using an enzyme-linked immunoabsorbent assay reader. The cell viability was expressed as a percentage of the corresponding control. The morphological differentiation assessed by phase contrast microscopy, by using an inverted microscope.

RESULTS

Characterization of CPHAp

SEM analysis shows a distinct nanostructural control of biomolecules in the biomimetic synthesis of CPHAp as shown in Fig. 1. XRD studies of synthesized CPHAp powder show formation of apatite phase; it seems that the presence of the varied biomolecules has not hindered the formation of HAp phase. Major peaks identified as shown in Fig. 2. The peak of α-calcium phosphate at 28.87 and 26.0119 is of the intensity 85% and 100% respectively.

FTIR spectroscopy analysis of CPHAp show bands at positions (1031 and 961/cm) which are assigned to symmetric P-O stretching. In addition, the bands at (1460, 1560, 1510, and 1430/cm) not very prominent, just like in the pure HAp, confirming very little or no protein. Bands at (1660, 1647/cm) represent bending mode of -OH group and band at 3435/cm represent stretching mode of the hydroxyl group, while 2360/cm band represents the carboxylic group. The band around 871/cm is typically for nucleation of HAp, and bands at (565, 517, 471/cm) stands for triply degenerated O-P-O bending and (418, 416/cm) bands correspond to doubly degenerate O-P-O bending mode as shown in Fig. 3.

Characterization of blank (CS-PVA-CPHAp) and encapsulated (CS-PVA-CPHAp-ATRA) biocomposites

Fig. 4 shows the SEM micrographs of PVA imposed CS/HAp blank, and ATRA encapsulated biocomposites. The results indicate that the PVA imposed CS/HAp biocomposite is composed of three-dimensional reticulate pores (Fig. 4a) and Fig. 4b nearly indicates that encapsulating ATRA to the PVA imposed CS/HAp biocomposite did not affect the network and porosity of the biocomposite.

As shown in Fig. 5, the spectra of ATRA itself and ion complexes between CS and ATRA were characterized at around 1252/cm. ATRA itself has specific (C-O stretch vibration) absorbance around 1252/cm and a significant decrease in the absorbance was observed according to the complex formation between CS and ATRA. Furthermore, the carbonyl group of ATRA characterized around 1690/cm decreased when ion complexes were formed between CS and ATRA. CPHAp absorption bands at 3160/cm and at about 602/cm. The band at 3160/cm is related to OH-stretching, which is attributed to the CPHAp functional group. However in ATRA loaded CS-PVA/HAp nanocomposite matrices the bands at 3160 is shifted to 3427/cm, 2417/cm (C-H stretching) is shifted to 2072/cm, 1647/cm (C-C stretching) is extended, 1402/cm is decreased are attributed to the interactions between PVA-CS-ATRA complex with HAp. The bands at 1170/cm and 1130/cm are attributed to P-O stretching while the bands close to 600/cm are related to P-O deformation vibrations of the PO4 three-group. The bands between 850 and 1000/cm are attributed to P-OH stretching. A characteristic band

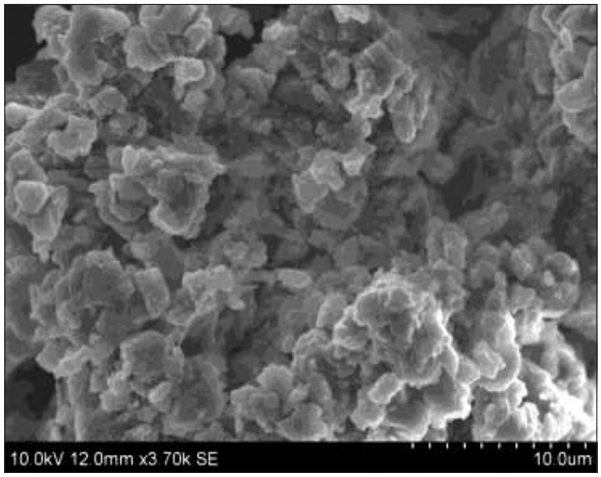

Fig. 1: Scanning electron microscopy micrograph showing controlled synthesis of hydroxyapatite nanoparticles using cucumber peel extract (CPHAp)

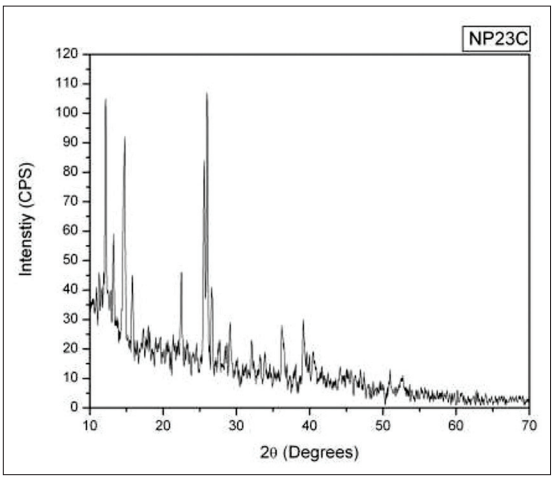

Fig. 2: X-ray diffraction patterns of CPHAp

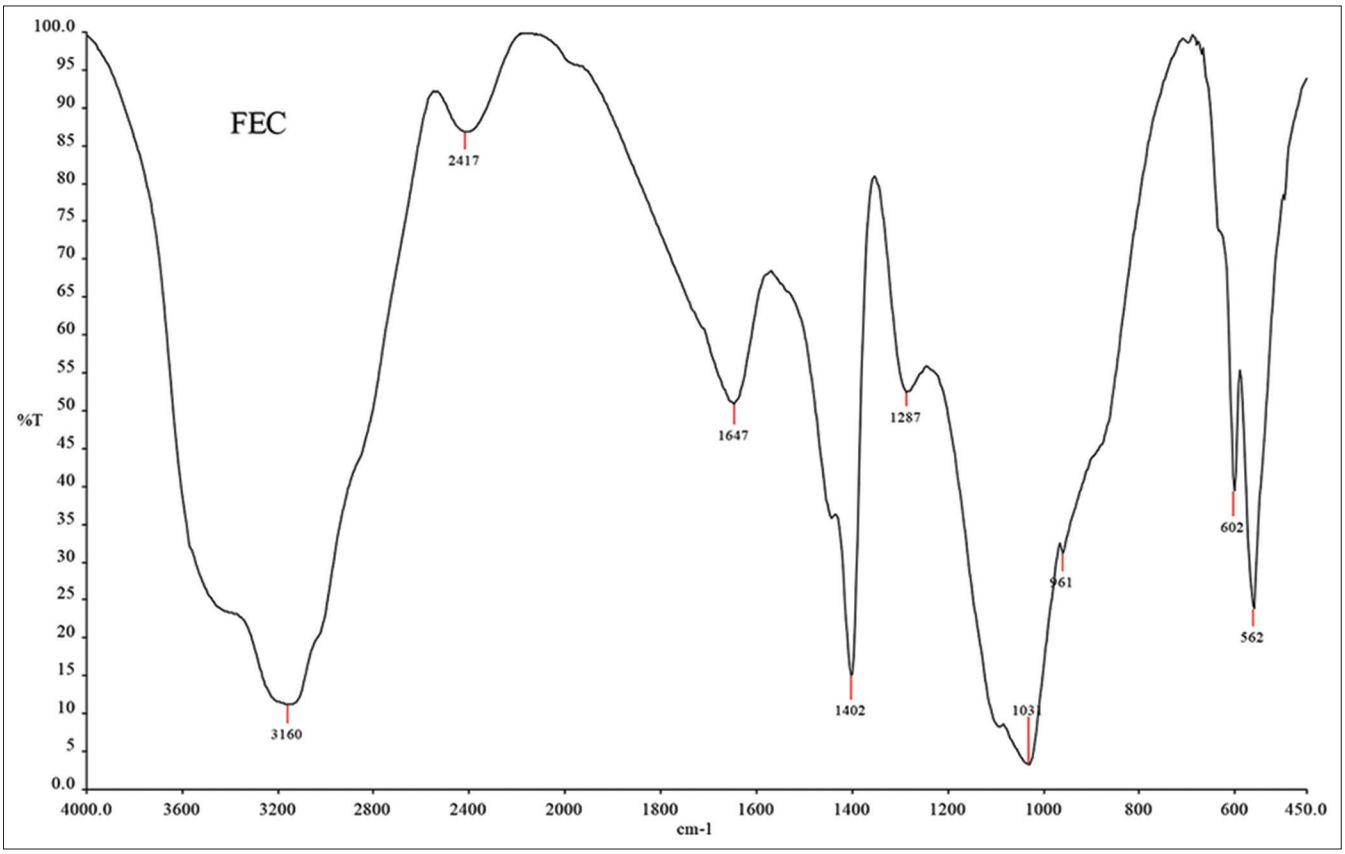

Fig. 3: Fourier transform infrared spectroscopy spectra of CPHAp

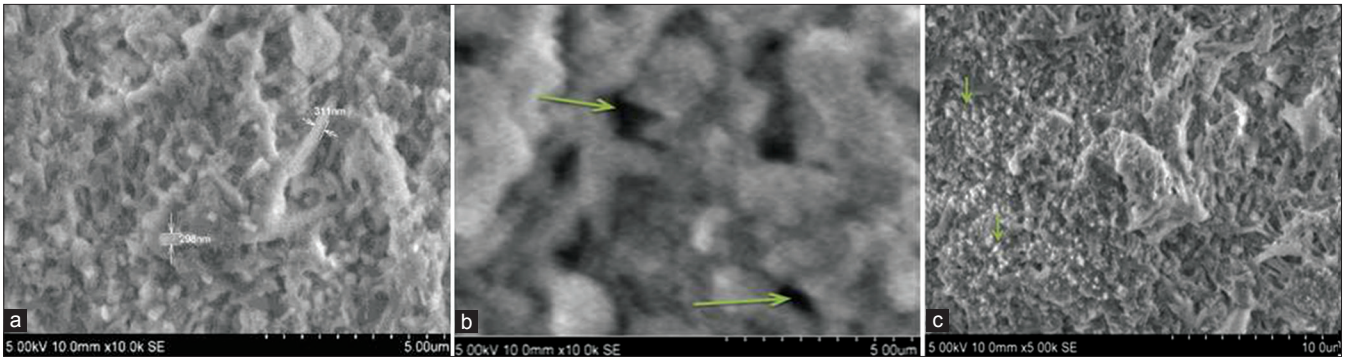

Fig. 4: Scanning electron microscopy images of, (a) Blank chitosan (CS)/polyvinyl alcohol (PVA) (CS-PVA-CPHAp), (b) further magnification into the CS-PVA-CPHAp scaffold and, (c) all-trans-retinoic acid (ATRA) loaded biocomposites (CS-PVA-CPHAp-ATRA)

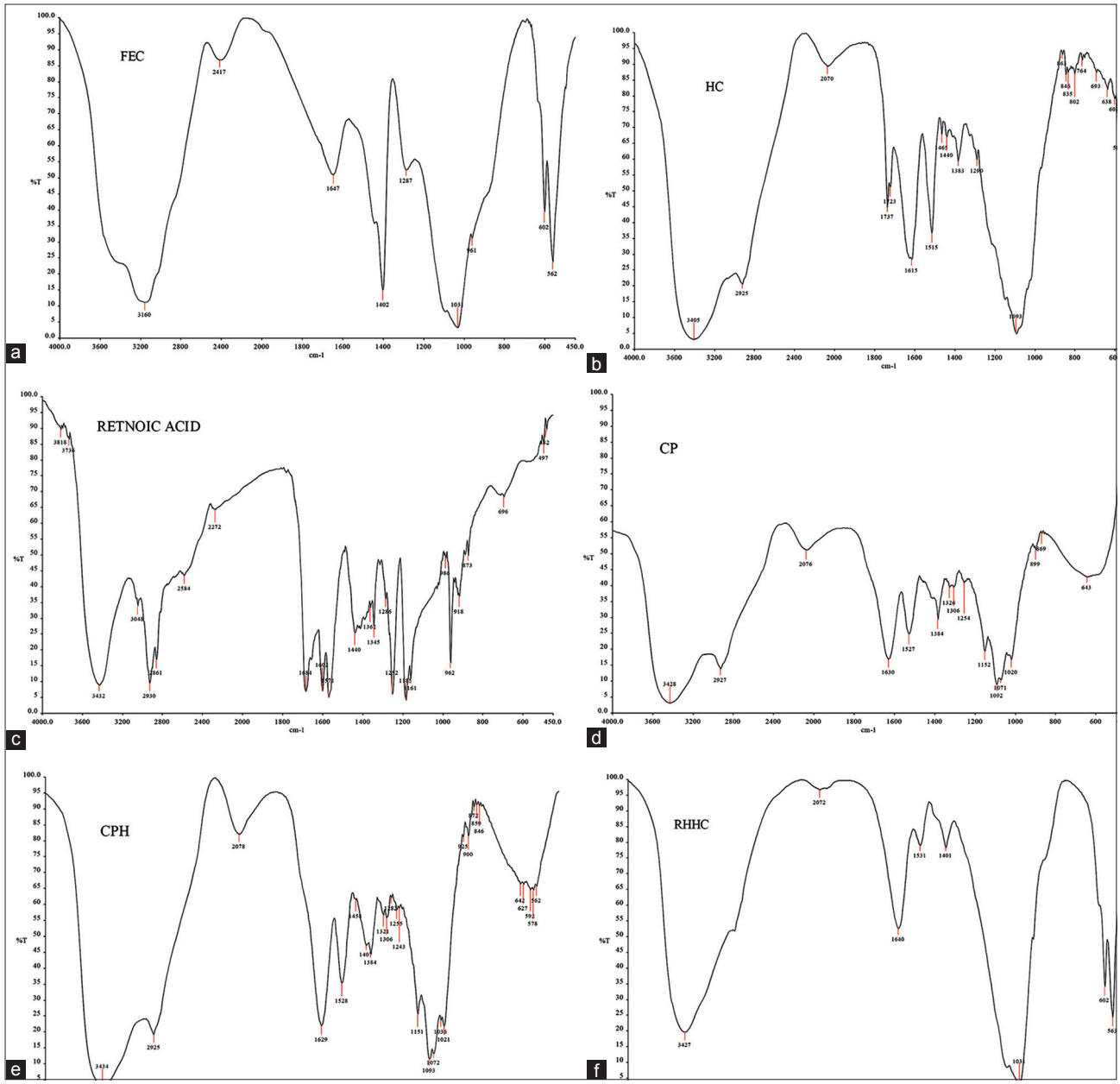

Fig. 5: Fourier transform infrared spectroscopy spectra of (a) CPHAp (b) chitosan CS (c) all-trans-retinoic acid (ATRA), (d) CS-polyvinyl alcohol (PVA), (e) CS-PVA-CPHAp (f) CS-PVA-CPHAp-ATRA

of CPHAp is visible at around 630/cm, which represents the OH end-group with lower steric impediment of the structure.

XRD pattern of CS, CPHAp, CS-CPHAp-ATRA and CS-PVA-CPHAp-ATRA biocomposites are shown in Fig. 6. Fig. 6a showed sharp crystalline peaks of CS at around 10° and 20° of 2q and Fig. 6b represents the diffraction patterns of CPHAp 28.87° and 26.0119°. When CPHAp was added to the CS solution with ATRA, the peaks are remained at the same position (Fig. 6c). While so, the disappearance of sharp crystalline peaks was observed in Fig. 6d when CPHAp was added to the CS-PVA solution with ATRA, indicating the intercalation structures have formed suggesting that the fabrication process promoted the amorphous state.

Actual amount of ATRA loaded in CS/HAp nanocomposite matrices

The ATRA-loaded sample was dissolved in 5 ml ACSF and the actual amount of ATRA was measured using a UV-Vis spectrometer at 280 nm. The actual drug ATRA amount contained in the sample was 67% when back calculated from the obtained data against a predetermined calibration curve of drugs. The calibration curve of ATRA was carried out in the concentration ranging from 0.002 mg/ml to 0.02 mg/ml.

***In vitro* release of ATRA from CS-PVA-CPHAp-ATRA**

Sustained release of all-trans retinoic acid from CS-PVA-CPHAp-ATRA was observed until 10 days, with the total amount of ATRA released at the end of 10 days being 55%.

Cell activity studies

The cytotoxicity of prepared biocomposites CS-PVA-CPHAp and CS-PVA CPHAp-ATRA to VERO cells was evaluated using MTT assay method. The results demonstrate the cell viability after 24hrs and 48 hrs incubation on medium with 30 nM ATRA release from biocomposite. The results present suggest that these biocomposites have generally low cytotoxicity to the VERO cells (Fig. 8a). Similar observations were noted from the phase contrast Microscopy evaluations of vero cells at 48 hrs of cell seeding on extract with 40 nM ATRA release from the CS-PVA CPHAp-ATRA biocomposite, further suggests that the scaffold is biologically active.

DISCUSSION

Food wastes and processing is a rich source of proteins and therefore may be viewed as a potential starting material for the production of high value-added products, including bionanocomposites [13].

Hence in the present study, we attempt to synthesis biogenic HAp from cucumber peel. The CPHAp formed using cucumber peel extract seen as clusters are made up of an assembly of particles of uniform shape and nanosize. The enoic acids present in the cucumber peel extract [14] has a strong affinity for calcium ions, which exerts the morphological control [12]. XRD studies could be indicative of the fact that the amount of compound extract added was sufficient for the entire HAp phase formation [12].

As part of our ongoing efforts toward the synthesis of biocomposites that are permissive for peripheral nerve innervations and regeneration of lost structures, we have initiated the study on synthesis of biogenic HAp/CS/PVA blends loaded with retinoic acid.

SEM of CS-PVA-CPHAp and CS-PVA CPHAp-ATRA showed highly interconnected porous structures with retinoic acid embedded on the surface of the CS-PVA-CPHAp biocomposite. The ATRA was uniformly spread throughout the surface, with few found to be agglomerated. Pore size and interconnectivity is a significant factor for cell attachment and spreading on scaffolds [15]. These observations suggest that this biocomposite is morphologically suitable for cell attachment and spreading.

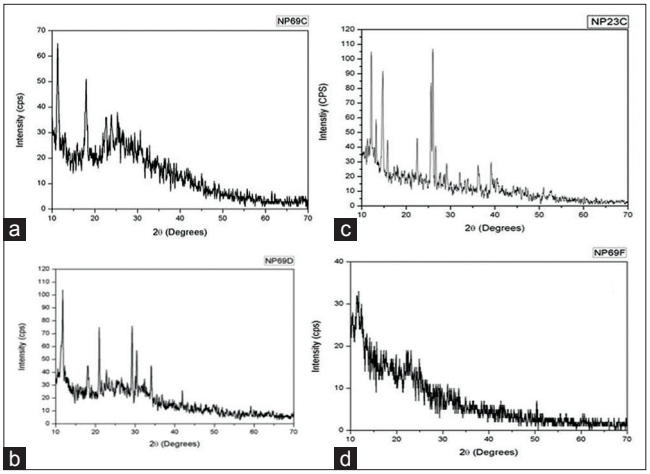

Fig. 6: X-ray diffraction patterns of, (a) Chitosan (CS), (b) CPHAp, (c) CS-CPHAp-all-trans-retinoic acid (ATRA) biocomposite, (d) CS-polyvinyl alcohol-CPHAp-ATRA biocomposite

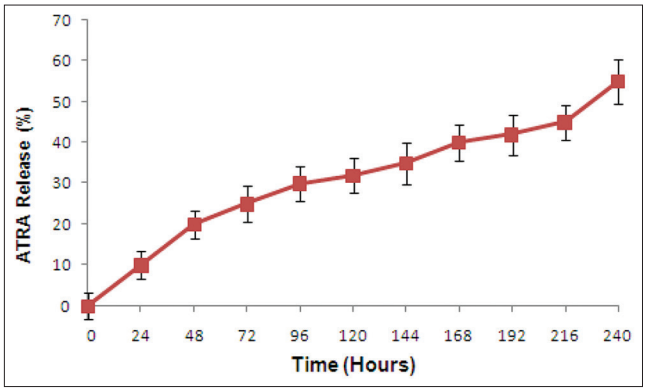

Fig. 7: Release profile of all-trans-retinoic acid (ATRA) in chitosan-polyvinyl alcohol-CPHAp-ATRA biocomposite

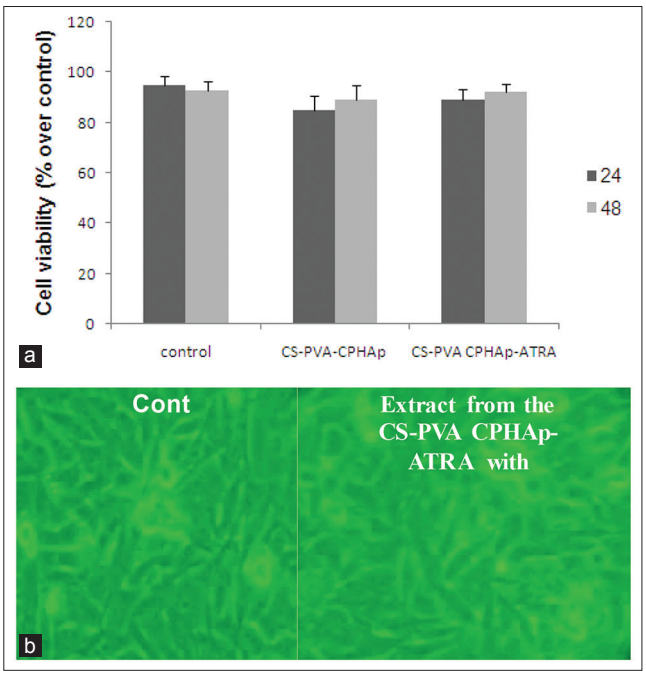

Fig. 8: (a)Cell viability measured at 24 hrs and 48 hrs of cell seeding on extract from the biocomposites. (b) Phase contrast microscopy evaluations of vero cells at 48 hrs of cell seeding on extract from the chitosan-polyvinyl alcohol CPHAp-all-trans-retinoic acid biocomposite

From the characteristic bands at corresponding wavelengths, FTIR spectra show that ATRA was encapsulated into the CS-PVA-CPHAp biocomposite not chemically altered and hence increases the potential of CS-PVA CPHAp-ATRA in releasing all-trans retinoic acid at the therapeutic site [9].

XRD analysis of CS-PVA CPHAp-ATRA suggests that the fabrication process promoted the amorphous state. This implies that encapsulation of ATRA into CS-PVA-CPHAp biocomposite improves the dissolution of ATRA and improves its drug targeting potential in craniofacial tissue engineering, which is preferred since retinoic acid is hydrophobic [16].

A sustained release of ATRA from CS-PVA CPHAp-ATRA is attributed to the entrapment of ATRA into CS-PVA-CPHAp by polyion complexation with CS [17], which is hydrogen bonded to PVA [18] and blended with CPHAp [10]. This acts as a barrier for the release of ATRA from bionanocomposite, which is desirable for therapeutic scaffolds.

Results from the MTT assay and Phase contrast microscopy evaluation demonstrates that the biocomposite with ATRA release of 30 nM does not impair the cell attachment and spreading [19], reliable proof of biocompatibility and non-cytotoxicity of scaffolds for tissue engineering.

Further CS-PVA CPHAp-ATRA biocomposite can provide microenvironment permissive for nerve regeneration as the concentration of the ATRA release from the biocomposite is within the range (4-40 nM) required to induce neurogenesis [20].

The environmentally friendly synthesis, fabrication process and therapeutic potential for CS-PVA CPHAp-ATRA biocomposite is highly reasoned for its use as a scaffold material in craniofacial tissue engineering.

CONCLUSIONS

This work dem onstrates the feasibility to prepare a biocomposite material incorporated with HAp, synthesized by biomimetic process utilizing biomolecules in cucumber peel. The proneurogenic factor, all-trans retinoic acid encapsulated in these biocomposite was released in a sustained manner. The fabrication process promoted the amorphous state to all-trans retinoic acid. The biocomposite CS-PVA CPHAp-ATRA was biocompatible and non-cytotoxic to vero cells. The release of ATRA from the biocomposite was within the range to induce neurogenesis. Therefore, the porous CS-PVA CPHAp-ATRA composites may be applied to craniofacial tissue engineering as a long-term or permanent scaffold due to their good biocompatibility and sustained release of proneurogenic factor.

AUTHORS' CONTRIBUTIONS

All the authors contribute equally to this work in co-coordinating and performing the experiments, writing the manuscript, design, interpretation and data analysis.

ACKNOWLEDGMENTS

The authors would like to thank Sathyabama University for providing the opportunity to carry out this research work.

REFERENCES

1. Hunt JA, Hobar PC. Common craniofacial anomalies: conditions of craniofacial atrophy/hypoplasia and neoplasia. Plast Reconstr Surg 2003;111:1497-508.
2. Zhu S, Zhang B, Man C, Ma Y, Hu J. NEL-like molecule-1-modified bone marrow mesenchymal stem cells/poly lactic-co-glycolic acid composite improves repair of large osteochondral defects in mandibular condyle. Osteoarthritis Cartilage 2011;19(6):743-50.
3. Susarla SM, Swanson E, Gordon CR. Craniomaxillofacial reconstruction using allotransplantation and tissue engineering: challenges, opportunities, and potential synergy. Ann Plast Surg 2011;67:655-61.
4. Blum N, Begemann G. Retinoic acid signaling controls the formation, proliferation and survival of the blastema during adult zebrafish fin regeneration. Development 2012;139(1):107-16.
5. Gupte MJ, Ma PX. Nanofibrous scaffolds for dental and craniofacial applications. J Dent Res 2012;91(3):227-34.
6. Weir MD, Xu HH. Osteoblastic induction on calcium phosphate cement-chitosan constructs for bone tissue engineering. J Biomed Mater Res A 2010;94(1):223-33.
7. Liu H, Peng H, Wu Y, Zhang C, Cai Y, Xu G, *et al*. The promotion of bone regeneration by nanofibrous hydroxyapatite/chitosan scaffolds by effects on integrin-BMP/Smad signaling pathway in BMSCs. Biomaterials 2013;34(18):4404-17.
8. Song W, Markel DC, Wang S, Shi T, Mao G, Ren W. Electrospun polyvinyl alcohol-collagen-hydroxyapatite nanofibers: a biomimetic extracellular matrix for osteoblastic cells. Nanotechnology 2012;23(11):115101.
9. Tan H, Chu CR, Payne KA, Marra KG. Injectable *in situ* forming biodegradable chitosan-hyaluronic acid based hydrogels for cartilage tissue engineering. Biomaterials 2009;30(13):2499-506.
10. Celebi H, Gurbuz M, Koparal S, Dogan A. Development of antibacterial electrospun chitosan/poly(vinyl alcohol) nanofibers containing silver ion-incorporated HAP nanoparticles. Special Issue: 15th European Conference on Composite Materials (ECCM15): Part 3. Compos Interfaces 2013;20(9):799-812.
11. Shuyan G, Zhengdao Li, Hongjie Z. Bioinspired green synthesis of nanomaterials and their applications. Curr Nanosci 2010;17:452-68.
12. Nayar S, Guha A. Waste utilization for the controlled synthesis of nanosized hydroxyapatite. Mater Sci Eng C 2009;29:1326-9.
13. Lancaster L, Lung MH, Sujan D. Utilization of agro-industrial waste in metal matrix composites: Towards sustainability. Int J Environ Earth Sci Eng 2013;7:1.
14. Mallik J, Akhter R. Phytochemical screening and *in-vitro* evaluation of reducing power, cytotoxicity and anti-fungal activities of ethanol extracts of *Cucumis sativus*. Int J Pharma Biol Arch 2012;3:555-60.
15. Peroglio M, Gremillard L, Gauthier C, Chazeau L, Verrier S, Alini M, *et al*. Mechanical properties and cytocompatibility of poly(e-caprolactone)-infiltrated biphasic calcium phosphate scaffolds with bimodal po re distribution. Acta Biomater 2010;6(11):4369-79.
16. Mohtaram NK, Junghuvk K, Carlson M, Stephanie MW. Nanofabrication of electrospun fibres for controlled release of retinoic acid. Proceedings of the 8th International Conference on Micro Manufacturing University of Victoria, Victoria, BC, Canada, March 25-28; 2013.
17. Jeong YI, Kim SH, Jung TY, Kim IY, Kang SS, Jin YH, *et al*. Polyion complex micelles composed of all-trans retinoic acid and poly (ethylene glycol)-grafted-chitosan. J Pharm Sci 2006;95:2348-60.
18. Erbin ZH, Meihua XI, Mingchun LI, Jiafu LI. Hydrogen bonding and compatibility of chitosan/polyvinyl alcohol blend films [J]. Chem Ind Eng Prog 2012;31:1082-7.
19. Okada Y, Shimazaki T, Sobue G, Okano H. Retinoic-acid-concentration-dependent acquisition of neural cell identity during *in vitro* differentiation of mouse embryonic stem cells. Dev Biol 2004;275(1):124-42.
20. Maia J, Santos T, Aday S, Agasse F, Cortes L, Malva JO, *et al*. Controlling the neuronal differentiation of stem cells by the intracellular delivery of retinoic acid-loaded nanoparticles. ACS Nano 2011;5(1):97-106.